

# Atomic resolution on MgO(001) by atomic force microscopy using a double quartz tuning fork sensor at low-temperature and ultrahigh vacuum

M. Heyde,<sup>a)</sup> M. Sterrer, H.-P. Rust, and H.-J. Freund

Fritz-Haber-Institut der Max-Planck-Gesellschaft, Faradayweg 4-6, D-14195 Berlin, Germany

(Received 11 March 2005; accepted 8 July 2005; published online 15 August 2005)

Atomic resolution with a double quartz tuning fork sensor for low-temperature ultrahigh vacuum atomic force and scanning tunneling microscopy is presented. The new features of the force sensor assembly are discussed. Atomically resolved images of MgO on Ag(001) have been obtained. Images acquired in the attractive and the repulsive regimes controlled to a constant frequency shift are shown, revealing contrast changes. © 2005 American Institute of Physics.

[DOI: 10.1063/1.2012523]

In this letter, we present atomically resolved frequency modulation (FM) atomic force microscopy (AFM) images of an ionic surface in the attractive and the repulsive regimes. Tip-induced surface distortion has been identified as an important component in the mechanism for contrast formation. Here, it is confirmed that atomic displacements strongly depend on the tip-surface separation. Atomic contrast in FM-AFM used with large amplitudes has been reported since 1995 on surfaces under ultrahigh vacuum.<sup>1-4</sup> The complexity of the experimental setup and difficulties in preparing clean, flat insulating, and semi-insulating surfaces have so far limited atomic resolution to only a few surfaces, such as NaCl and several other alkali halides,<sup>5</sup> TiO<sub>2</sub>,<sup>6</sup> CaF<sub>2</sub>,<sup>7</sup> and Al<sub>2</sub>O<sub>3</sub>(0001).<sup>8</sup> Recently, atomically resolved images have appeared for MgO(001).<sup>9</sup> However, the number of atomically resolved images with small-amplitude FM-AFM in ultrahigh vacuum is still small and has only been shown by Giessibl *et al.*<sup>10-12</sup> so far.

Atomically resolved images utilizing a double quartz tuning fork sensor driven at small oscillation amplitudes in the range of about 0.5 nm are presented. All AFM experiments have been performed in ultrahigh vacuum at a temperature of 5 K using a custom-built instrument. The sensor has been described in detail in Ref. 13. The sensor has a resonance frequency  $f_0 = 17\,444$  Hz, a  $Q$  factor of 12 500, and an estimated stiffness of  $k = 30\,000$  N/m. A cut Pt/Ir wire with a diameter of 0.25 mm has been used as a tip. The tip is electrically connected by a thin Pt/Rh wire with a diameter of 50  $\mu\text{m}$ . Both, the tip and Pt/Rh wire are insulated from the tuning fork electrodes. The double tuning fork assembly is operated by the sensor controller/FM-detector easyPLLplus from Nanosurf<sup>14</sup> in the self-exciting oscillation mode. The principle of frequency detection was described by Albrecht *et al.*<sup>15</sup> A unit by Nanotech Electronics<sup>16</sup> was used for scan control and data acquisition.

For stable recording of high-resolution images, one needs to take care of the nonmonotonic force feedback signal.<sup>12,17</sup> In general, the force is attractive for large distances and, upon decreasing the distance between tip and sample, the force turns repulsive causing a frequency shift which is proportional to the integral of the force. A typical frequency shift curve over  $z$  displacement is given in Fig. 1 by the dashed line. A typical set point for obtaining stable

FM-AFM operation is to work on the attractive part of the tip-surface interaction curve (point  $a'$ ). If the tip suddenly encounters a much less attractive or a repulsive interaction, the feedback electronics would move the tip closer to the surface searching for stronger attraction. This often leads to the tip crashing into the surface. It can be provoked by surface defects, adsorbed species, or by fluctuations in the amplitude of the tuning fork vibration. The black line in Fig. 1 represents the rectified frequency shift signal,<sup>18</sup> which is used as feedback signal in our setup. With such a setup, tip crashes can be avoided. Point  $a$  marks a set point for the tip-sample distance in the attractive regime. If the frequency shift reaches point  $b$ , e.g., as a result of fluctuations, the set point will jump to point  $c$ . By changing the offset of the frequency shift as well as the set point itself, different points ( $c'$ ,  $d'$ ,  $e'$ ) can be accessed for imaging in the repulsive regime. With such a setup stable feedback in the attractive and the repulsive part can be obtained.

The sample used in these experiments is a thin MgO film grown on Ag(001). The study of thin metal oxide films pursues several goals. Ultrathin films allow comparison between force microscopy and simultaneously performed tunneling microscopy. Finally, the use of thin films is a way of circumventing the problems associated with the charging of insulating materials. The single-crystal Ag(001) surface was cleaned by several cycles of ion sputtering (Ar<sup>+</sup>, 10  $\mu\text{A}$ , 800

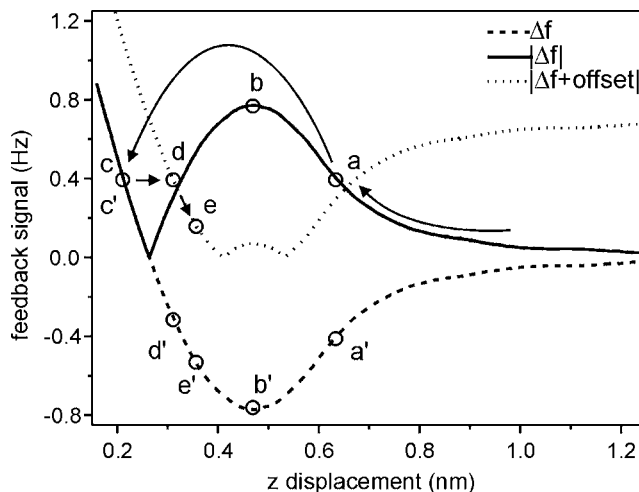


FIG. 1. Schematic of the frequency shift, rectified frequency shift, and rectified frequency shift plus offset over  $z$  displacement is given.

<sup>a)</sup>Electronic mail: heyde@fhi-berlin.mpg.de

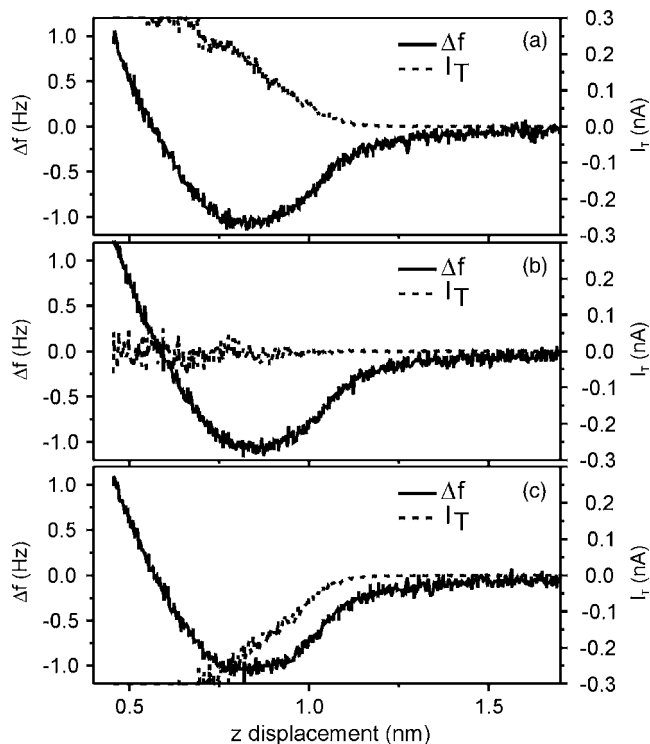


FIG. 2. Plot of tunneling current  $I_T$  (dashed line) and frequency shift  $\Delta f$  (solid line) as a function of the  $z$  displacement measured at sample voltages (a)  $V_S=0.1$  mV, (b)  $V_S=0$  mV, and (c)  $V_S=-0.1$  mV.

V) and annealing (700 K). This system exhibits a small lattice mismatch between MgO and the metal substrate of 2.9%. The MgO/Ag(001) films were prepared by electron-beam evaporating Mg in an oxygen background pressure of  $5 \times 10^{-7}$  using deposition rates of  $0.75 \text{ ML min}^{-1}$ . Typically MgO films of 4 monolayers (ML) have been prepared. It is a question of definition to decide what thickness is needed to call a film insulating. Tunneling spectra of ultrathin MgO films reveal that the electronic structure of the bulk material already appears in the first ML, and that three atomic layers essentially resemble the properties of a bulk system.<sup>19</sup>

A set of tunneling current and frequency shift curves as a function of  $z$  displacement acquired at different bias voltages has been plotted in Fig. 2 to characterize the performance of the double tuning fork sensor. Large bias voltages between tip and sample give rise to a long-range attractive force and changes the imaging conditions. An example is the bias dependence of AFM images and the tunneling current variations on semiconductor surfaces which has been recently presented.<sup>20</sup> Here, at low bias voltages, we wanted to avoid the influence of tunneling current on the frequency shift. Therefore, the proof is the simultaneous acquisition of frequency shift and tunneling current over the  $z$  displacement at small positive, zero, and negative sample voltages. The data in Fig. 2(a) was acquired at a sample voltage of  $V_S=+0.1$  mV, where the tunneling current shows an increase with a decreasing  $z$  displacement. By setting the bias voltage to zero [Fig. 2(b)], the tunneling current shows only an increase of noise with decreasing  $z$  displacement. At a sample voltage of  $V_S=-0.1$  mV, the tunneling current shows an increase in the negative direction with a decreasing  $z$  displacement. The frequency shift curves are unperturbed by the sample bias voltage. This experiment shows that our force sensor is free from tunneling current contribution.

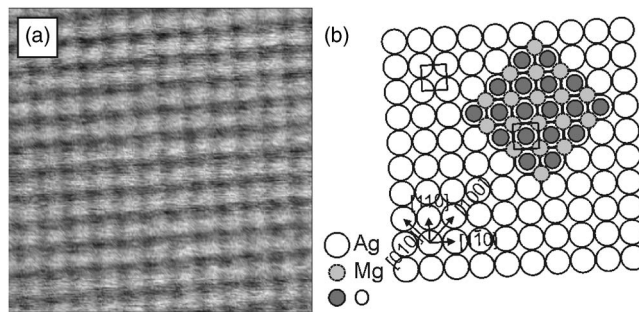


FIG. 3. (a) FM-AFM image of MgO on Ag(001) with atomic resolution. Scan area  $3.5 \text{ nm}$  by  $3.5 \text{ nm}$ ,  $\Delta f=-3.8 \text{ Hz}$ , oscillation amplitude  $A=0.35 \text{ nm}$ ,  $T=5 \text{ K}$ , approximately  $13 \text{ pm}$  corrugation. (b) The MgO/Ag(001) growth model, schematic illustration of the configuration: Mg-atoms occupy hollow sites, i.e., they continue the Ag face-centered-cubic lattice ( $a=0.409 \text{ nm}$ ), O atoms occupy on top sites. The Ag(001) surface unit cell is indicated.

Figure 3 shows an image with atomic resolution which was obtained on a flat terrace of the MgO film. The direction of largest differences in contrast corresponds to the distance of next-neighbor ions in the [001] direction. The corrugation is in the range of about  $13 \text{ pm}$ . It strongly depends on the relation between short- and long-range forces, which itself depends on the sharpness of the tip and the frequency shift set point. Nevertheless, the determined height corrugation is comparable with the values of numerical simulations recently done on MgO(001).<sup>21</sup> Generally, in force microscopy of ionic surfaces, e.g., NaCl,<sup>22</sup> KBr,<sup>23</sup> and MgO,<sup>9</sup> only one type of ion is imaged as a protrusion. The self-evident interpretation of this finding is a strong variation in the short-range forces above anions and cations. The range of frequency shift for which atomic resolution can be obtained is normally limited. The enhancement of the contrast due to displacement of ions by the force of the tip is most prominent for increasing frequency shifts. Further increase in the frequency shift causes a displacement of ions which develops into instability and usually causes ions to jump from the sample surface to the tip. This abrupt change in the tip-surface interaction is likely to produce a jump in the imaging parameters from the attractive to the repulsive mode. Figure 4(a) shows a high-resolution image acquired in the attractive mode, while Fig. 4(b) the same area imaged in the repulsive mode. A grid indicates the position of equivalent ionic species. The switching between the attractive and the repulsive mode has been performed on purpose by adjusting the fre-

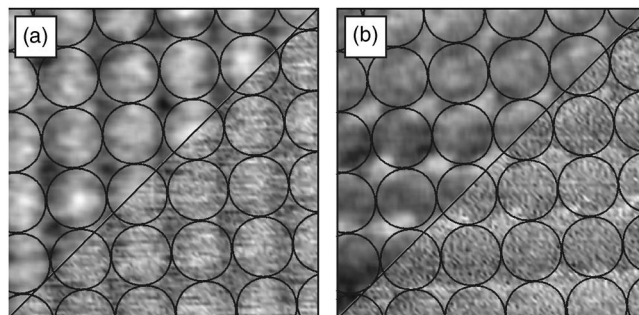


FIG. 4. FM-AFM image of MgO on Ag(001) with atomic resolution. The lower right part in each image shows the unfiltered raw data, the upper left part are low pass filtered. Scan area  $1.5 \text{ nm}$  by  $1.5 \text{ nm}$ , oscillation amplitude  $A=0.35 \text{ nm}$ ,  $T=5 \text{ K}$ , (a) attractive regime  $\Delta f=-3.7 \text{ Hz}$ , and (b) repulsive regime  $\Delta f=+3.7 \text{ Hz}$ .

quency shift set point. This experiment has been repeated several times and the obtained data have shown the same conversion in the imaging contrast. As predicted by theory<sup>24</sup> and recently shown for CaF<sub>2</sub><sup>12</sup> a change in the imaging contrast can be observed in the repulsive mode. This result emphasizes the importance of the tip-induced relaxation of the surface ions in the tip-surface interaction and in image contrast. If the Pt/Ir tip is contaminated by some MgO, one can expect to have an O- or Mg-terminated nanotip. For a chosen Mg-terminated nanotip, the minima in the attractive mode image [Fig. 4(a)] would correspond to surface magnesium, and the maxima to surface oxygen. Please note that an O-terminated tip would produce inverted results. Above a Mg site with a Mg-terminated nanotip, the force is attractive until it becomes repulsive at a close enough distance. The attractive force above an O site is calculated to be much larger than that above Mg sites, which determines the corrugation in the attractive mode.<sup>25</sup> By imaging in the repulsive mode, the repulsive force above the Mg sites is stronger than the force contribution due to the O sites. For a Mg-terminated nanotip in the repulsive mode, the minima would correspond to surface oxygen and the maxima to surface magnesium. This might explain the change in contrast between attractive and repulsive modes in the FM-AFM images of the same area (Fig. 4). However, the contrast in the repulsive mode seems to be dominated by the repulsion of the surface ions. Due to a more complicated inward displacement, a lateral inplane distortion of the surface ions must be considered in addition, when the repulsive force between the tip and surface is originated. At such a close approach, the situation becomes even more complicated due to substantial deformation of many atoms both at the tip end and at the surface underneath it. So, not only the influence of the sublattice has to be taken into account, but also the tip apex itself might contribute a modified symmetry to the image contrast.

In conclusion, we have shown that our double tuning fork sensor operated in an ultrahigh vacuum at low temperature and at small oscillation amplitudes is capable of atomic resolution. For all images, the tip-sample distance has been

controlled to a constant frequency shift both in the attractive and repulsive modes. The theory for the inversion in contrast when switching from attractive to repulsive imaging has been explained and verified experimentally for MgO.

<sup>1</sup>F. J. Giessibl, *Science* **267**, 68 (1995).

<sup>2</sup>K. S. Kitamura and M. Iwatsuki, *Jpn. J. Appl. Phys., Part 2* **34**, L145 (1995).

<sup>3</sup>Y. Sugawara, M. Ohta, H. Ueyama, and S. Morita, *Science* **270**, 1646 (1995).

<sup>4</sup>W. Allers, A. Schwarz, U. D. Schwarz, and R. Wiesendanger, *Rev. Sci. Instrum.* **69**, 221 (1998).

<sup>5</sup>M. Bammerlin, R. Lüthi, E. Meyer, A. Baratoff, J. Lü, M. Guggisberg, C. Loppacher, C. Gerber, and H.-J. Güntherodt, *Appl. Phys. A: Mater. Sci. Process.* **66**, S293 (1998).

<sup>6</sup>K. Fukui, H. Onishi, and Y. Iwasawa, *Phys. Rev. Lett.* **79**, 4202 (1997).

<sup>7</sup>M. Reichling and C. Barth, *Phys. Rev. Lett.* **83**, 768 (1999).

<sup>8</sup>C. Barth and M. Reichling, *Nature (London)* **414**, 54 (2001).

<sup>9</sup>C. Barth and C. R. Henry, *Phys. Rev. Lett.* **91**, 196102 (2003).

<sup>10</sup>F. J. Giessibl, *Appl. Phys. Lett.* **76**, 1470 (2000).

<sup>11</sup>S. Hembacher, F. J. Giessibl, J. Mannhart, and C. F. Quate, *Phys. Rev. Lett.* **94**, 056101 (2005).

<sup>12</sup>F. J. Giessibl and M. Reichling, *Nanotechnology* **16**, S118 (2005).

<sup>13</sup>M. Heyde, M. Kulawik, H.-P. Rust, and H.-J. Freund, *Rev. Sci. Instrum.* **75**, 2446 (2004).

<sup>14</sup>Nanosurf AG, Grammetstrasse 14, CH-4410 Liestal, Switzerland.

<sup>15</sup>T. R. Albrecht, P. Grütter, D. Horne, and D. Rugar, *J. Appl. Phys.* **69**, 668 (1991).

<sup>16</sup>Nanotec Electronica, Parque Científico de Madrid, Pabellon C, campus UAM, Cantoblanco, E-28049 Madrid, Spain.

<sup>17</sup>F. J. Giessibl, *Rev. Mod. Phys.* **75**, 949 (2003).

<sup>18</sup>H. Ueyama, Y. Sugawara, and S. Morita, *Appl. Phys. A: Mater. Sci. Process.* **66**, S295 (1998).

<sup>19</sup>S. Schintke, S. Messerli, M. Pivetta, F. Patthey, L. Libioulle, M. Stengel, A. D. Vita, and W. D. Schneider, *Phys. Rev. Lett.* **87**, 276801 (2001).

<sup>20</sup>T. Arai and M. Tomitori, *Appl. Surf. Sci.* **157**, 207 (2000).

<sup>21</sup>A. I. Livshits, A. L. Shluger, A. L. Rohl, and A. S. Foster, *Phys. Rev. B* **59**, 2436 (1999).

<sup>22</sup>R. Bennowitz, A. S. Foster, L. N. Kantorovich, M. Bammerlin, C. Loppacher, S. Schär, M. Guggisberg, E. Meyer, and A. L. Shluger, *Phys. Rev. B* **62**, 2074 (2000).

<sup>23</sup>R. Bennowitz, S. Schär, E. Gnecco, O. Pfeiffer, M. Bammerlin, and E. Meyer, *Appl. Phys. A: Mater. Sci. Process.* **78**, 837 (2004).

<sup>24</sup>A. S. Foster, C. Barth, A. L. Shluger, R. M. Nieminen, and M. Reichling, *Phys. Rev. B* **66**, 235417 (2002).

<sup>25</sup>L. N. Kantorovich, A. L. Shluger, and A. M. Stoneham, *Phys. Rev. B* **63**, 184111 (2001).